Inorganica Chimica Acta 405 (2013) 415–426

Contents lists available at SciVerse ScienceDirect

Inorganica Chimica Acta

journal homepage: www.elsevier.com/locate/ica

Synthesis, spectral, X-ray crystallography, electrochemistry, DNA/protein binding and radical scavenging activity of new palladium(II) complexes containing triphenylarsine

P. Kalaivani [a], R. Prabhakaran [a,*], M.V. Kaveri [a], R. Huang [b], R.J. Staples [b], K. Natarajan [a,*]

[a] Department of Chemistry, Bharathiar University, Coimbatore 641 046, India
[b] Department of Chemistry, Michigan State University, East Lansing, MI 48824, USA

ARTICLE INFO

Article history:
Received 9 May 2013
Received in revised form 24 June 2013
Accepted 24 June 2013
Available online 2 July 2013

Keywords:
Palladium(II) complexes
Thiosemicarbazones
X-ray crystallography
Electrochemistry
DNA/protein binding
Radical scavenging activity

ABSTRACT

The reactions of $[PdCl_2(AsPh_3)_2]$ with equimolar amount of salicylaldehyde-4(N)-phenylthiosemicarbazone [H_2-(Sal-ptsc)] (H_2L^1) and 2-hydroxy-1-naphthaldehyde-4(N)-methylthiosemicarbazone [H_2-(Nap-mtsc)] (H_2L^2) were carried out in ethanol/dichloromethane medium. The obtained products (**1** and **2**) were characterized by variours spectral and analytical techniques. From the X-ray crystallographic studies, it is inferred that both the ligands coordinate as ONS tridentate dibasic donor by forming more common five and six member chelate rings. The complex **1** crystallizes in the triclinic space group $P\bar{1}$ with two molecules per unit cell, has the dimensions of $a = 10.1680(12)$ Å, $b = 10.5535(12)$ Å, $c = 13.3852(15)$ Å, $\alpha = 78.9980(10)°$, $\beta = 82.7610(10)°$ and $\gamma = 86.2490(10)°$. The complex **2** crystallizes in the monoclinic space group $P2(1)/n$ with four molecules per unit cell, has the dimensions of $a = 14.0981(3)$ Å, $b = 11.2881(2)$ Å, $c = 18.2678(3)$ Å, $\alpha = 90°$, $\beta = 111.00(10)°$ and $\gamma = 90°$. The complexes **1** and **2** have been tested for their binding towards Herring Sperm (HS)-DNA and BSA (bovine serum albumin). The new complexes bound to DNA by electrostatic binding mode and they had a strong binding affinity with BSA. The mechanism of quenching was found as static. In addition, the free radical bleaching ability of complexes with DPPH (1,1-diphenyl-2-picryl-hydrazyl) radical was carried out.

1. Introduction

The chemistry of thiosemicarbazones has gained importance because of their simple preparation, unpredictable complexation properties and their pharmacological applications [1]. The coordinating ability of thiosemicarbazones is attributed to the extended delocalization of electron density over the –NH–C(S)–NH–N = system, which is enhanced by substitution on the terminal nitrogen [1b,2–6]. Variation in the substitution on the azomethine (C2) carbon of the thiosemicarbazone ligands influences the mode of their binding. On introduction of nitrogen and/or oxygen containing substituents on azomethine carbon, it is anticipated that the binding ability of thiosemicarbazone becomes more capricious. The study of the interaction of transition metal complexes with DNA is a vibrant area of research [7]. The ability to selectively target and cleave DNA with high affinity and to report on the binding event by changes in luminescence is of great current interest [8]. An advantage of using transition metal complexes in such studies can be conveniently varied to suit individual applications. This may be due to their ability to inhibit the biosynthesis of DNA, possibly by binding with nitrogen base pair of DNA or RNA, which may hinder or block base replication [9]. In addition, palladium(II) thiosemicarbazones possess interesting antiproliferative effects on human cancer cell lines, including tumor cell lines resistant to cisplatin [10–13] and have also exhibited good antimycobacterial effects [14]. In continuation with our investigation [15–25] herein we report the reactions of salicylaldehyde-4(N)-phenylthiosemicarbazone (H_2L^1) and 2-hydroxy-1-naphthaldehyde-4(N)-methylthiosemicarbazone [(H_2L^2) with palladium(II) complexes containing triphenylarsine and their DNA and protein interactions.

2. Experimental section

2.1. Materials and methods

The ligands [H_2-(Sal-ptsc)] (H_2L^1), [H_2-(Nap-mtsc)] (H_2L^2) and palladium metallic precursor $[PdCl_2(AsPh_3)_2]$ were synthesized according to the standard literature procedures [26,27]. All the reagents used in this study were analar grade and the solvents were purified and dried according to the standard procedure [28]. HS-DNA, ethidium bromide (EB) and BSA were obtained from Sigma Aldrich and used as received. Infrared spectra were measured as

* Corresponding authors. Tel.: +91 422 2428319; fax: +91 422 2422387.
E-mail addresses: rpnchemist@gmail.com (R. Prabhakaran), k_natraj6@yahoo.com (K. Natarajan).

0020-1693/$ - see front matter © 2013 Elsevier B.V. All rights reserved.
http://dx.doi.org/10.1016/j.ica.2013.06.038

KBr pellets on a Nicolet Avatar Model FT-IR spectrophotometer in the 400–4000 cm^{-1} range. Elemental analyses of carbon, hydrogen, nitrogen, and sulfur were determined using Vario EL III CHNS at the Department ofChemistry, Bharathiar University, Coimbatore, India. The electronic spectra of the complexes have been recorded in dichloromethane using a Systronics 119 Spectrophotometer in the 800–200 nm range. ^1H and ^{13}C NMR spectra were taken in DMSO at room temperature with a Bruker 400 MHz instrument with chemical shift relative to tetramethylsilane. Cyclic voltammograms were recorded on a CH instrument by using platinum wire working electrode and platinum disc counter electrode. All the potentials were referenced to the standard Ag/AgCl electrode and ferrocene was used as external standard. Melting points were recorded by using Lab India melting point apparatus.

2.2. Synthesis of the ligands

2.2.1. Synthesis of salicylaldehyde-4(N)-phenylthiosemicarbazone, [H_2-(Sal-ptsc)](H_2L^1) [26]

A 4.2 g (0.025 mol) of 4(N)-phenylthiosemicarbazide was dissolved in 20 cm^3 of hot ethanol and to this was added 2.7 g of (0.025 mol) salicylaldehyde in 10 cm^3 of ethanol over a period of 10 min with continuous stirring. The reaction mixture was further refluxed for 5 h and allowed to cool whereby a shining yellow compound began to separate which was filtered and washed thoroughly with ethanol and then dried *in vacuum*. The compound was recrystallized from hot ethanol. The product dissolves in common organic solvents such as acetone, methanol, ethanol, dichloromethane, chloroform, DMF and DMSO. Yield: 80%. M.p. 191 °C. *Anal.* Calc. for $C_{14}H_{13}N_3OS$: C, 61.97; H, 4.83; N, 15.49; S, 11.82. Found: C, 61.91; H, 4.79; N, 15.42; S, 11.78%. FT-IR (cm^{-1}) in KBr: 3419 (ν_{OH}), 1620 ($\nu_{C=N}$), 1270(ν_{C-O}), 815 ($\nu_{C=S}$); ^1H NMR (DMSO-d6, ppm): 11.40 (s, 1H, OH), 10.01 (s, 1H, NHCS), 9.59 (s, 1H, NHPh), 8.33 (s, 1H, CH=N), 6.79–7.58 (m, aromatic); ^{13}C NMR (DMSO-d6, ppm): 186.4 (C=S), 162.28 (C=N), 152.1 (C-2, aromatic), 132.08 (C-4, aromatic), 128.92 (C-11, C-13, aromatic), 123.7 (C-10, C-14, aromatic), 117.4 (C-5, aromatic), 112.0 (C-3, aromatic).

2.2.2. Synthesis of 2-hydroxy-1-naphthaldehyde-4(N)-methylthiosemicarbazone, [H_2-(Nap-mtsc)](H_2L^2) [26]

The method above described was followed for the preparation. The ligand [H_2-(Nap-mtsc)] was prepared from 4(N)-methylthiosemicarbazide (2.63 g, 0.025 mol) and 2-hydroxy-1-naphthaldehyde (4.30 g, 0.025 mol). A cream white compound began to separate out. Yield: 78%. M.p. 220 °C. *Anal.* Calc. for $C_{13}H_{13}N_3OS$: C, 60.21; H, 5.05; N, 16.20; S, 12.36. Found: C, 60.17; H, 4.99; N, 16.14; S, 12.31%. FT-IR (cm^{-1}) in KBr: 3423 (ν_{OH}), 1640 ($\nu_{C=N}$), 1250 (ν_{C-O}), 795 ($\nu_{C=S}$); ^{1}HNMR (DMSO-d6, ppm): 11.25 (s, 1H, OH), 10.65 (s, 1H, NHCS), 9.10 (s, 1H, $NHCH_3$), 8.02 (s, 1H, CH=N), 7.07–7.71 (m, 3H, aromatic), 2.50 (d (J = 2.4), 3H, CH_3); ^{13}C NMR (DMSO-d6, ppm): 181.4 (C=S), 157.24 (C=N), 135.12 (C-4, aromatic), 129.15 (C-6, aromatic), 126.4 (C-8, C-9, aromatic), 122.82 (C-1, aromatic), 118.19 (C-3, aromatic), 28.6 (CH_3).

2.3. Synthesis of [Pd(Sal-ptsc)($AsPh_3$)] (**1**)

An ethanolic (25 cm^3) solution of [$PdCl_2(AsPh_3)_2$] (0.200 g; 0.253 mmol) was slowly added to salicylaldehyde-4(N)-phenylthiosemicarbazone (H_2L^1) (0.068 g; 0.253 mmol) in dichloromethane (25 cm^3). The mixture was allowed to stand for 4 days at room temperature. Orange red crystals obtained were filtered, washed with n-hexane and dried. Yield: 52%. M.p. 218 °C. *Anal.* Calc. for $C_{32}H_{26}N_3OSPdAs$: C, 56.36; H, 3.84; N, 6.16; S, 4.70. Found: C, 56.30, H, 3.80; N, 6.13; S, 4.62 . FT-IR (cm^{-1}) in KBr: 1583 ($\nu_{C=N}$), 1342(ν_{C-O}), 743 (ν_{C-S}), 1440, 1070, 691 cm^{-1} (for $AsPh_3$) ; UV–Vis (CH_2Cl_2), λ_{max}: 240, 272 nm (intra-ligand transition); 320, 380 nm (LMCT s → d); 440 nm (MLCT); ^1H NMR (DMSO-d6, ppm): δ 8.6 (s, 1H, CH=N), 9.6 (s, terminal –NH), 6.7–7.8 (m, aromatic); ^{13}C NMR (DMSO-d6, ppm): 166.4 (C–S), 162.24 (C=N), 153.6 (C-2 Aromatic), 152.1 (aromatic $AsPh_3$), 132.08 (aromatic $AsPh_3$), 129.15 (aromatic, $AsPh_3$), 127.6 (C-11, C-13, aromatic), 126.6 (C-6,aromatic), 121.7 (C-5, aromatic), 115.1 (C-10, C-14 aromatic), 112.0 (C-1, aromatic).

The very similar method was followed to synthesize the following complex.

2.4. Synthesis of [Pd(Nap-mtsc)($AsPh_3$)] (**2**)

It was prepared by the procedure as has been used for (**1**) with naphthaldehyde-4(N)-methylthiosemicarbazone [H_2-(Nap-mtsc)] (0.066 g; 0.253 mmol). Evaporation of the solvent mixture gave an orange solid which was dissolved in dichloromethane and subjected to column chromatography. A yellowish orange band was isolated with benzene and on evaporation yielded orange compound. It was recrystallised from hot dimethylformamide which afforded reddish orange crystals. Yield: 68%. M.p. 260 °C. *Anal.* Calc. for $C_{31}H_{26}N_3OSPdAs$: C, 55.58; H, 3.91; N, 6.27; S, 4.79. Found:C, 55.49; H, 3.87; N, 6.18; S, 4.20%. FT-IR (cm^{-1}) in KBr: 1616 ($\nu_{C=N}$), 1259(ν_{C-O}), 738 (ν_{C-S}), 1428, 1074, 688 cm^{-1} (for $AsPh_3$) ; UV–Vis (CH_2Cl_2), λ_{max}: 254, 270 nm (intra-ligand transition); 318, 380 nm (LMCT s → d); 430 nm (MLCT); ^1H NMR (DMSO-d6, ppm): δ 8.07 (d (J = 11.2), CH=N), 9.29 (s, terminal –NH), 2.84 (d (J = 3.6), –CH_3), 6.80–7.99 (m, aromatic); ^{13}C NMR (DMSO-d6, ppm): 163.4 (C–S), 158.24 (C=N), 155.6 (aromaticAsPh_3), 151.4 (aromatic $AsPh_3$), 130.12 (aromatic $AsPh_3$), 129.15 (C-5, aromatic), 126.6 (C-8, C-9, aromatic), 123.7 (C-7, aromatic), 118.02 (C-1, aromatic), 28.8 (CH_3).

2.5. Single crystal X-ray crystallography

Single crystals of [$PdCl_2(AsPh_3)_2$], [Pd(Sal-ptsc)($AsPh_3$)] (**1**) and [Pd(Nap-mtsc)($AsPh_3$)] (**2**) were obtained from C_6H_6/CH_3CN, C_2H_5OH/CH_2Cl_2 mixture and DMF respectively. Single crystal data collections and corrections were done at 173 K with Bruker SMART 1000 CCD using graphite mono chromated Mo Kα (λ = 0.71073 Å) radiation. The structural solution were done by using SHELXS-97 [29] and refined by full matrix least square on F^2 using SHELXL-97 [30].

2.6. DNA binding study

HS-DNA solutions of various concentrations (0.05-0.5 μM) dissolved in a tris HCl buffer (pH 7) were added to the palladium complexes **1** and **2** (1 μM dissolved in DMSO/H_2O mixture). Absorption spectra were recorded after equilibrium at 20 °C for 10 min. The intrinsic binding constant K_b was determined by using Stern Volmer Eq. (1) [31,32].

$$[DNA]/[\varepsilon_a - \varepsilon_f]) = [DNA]/[\varepsilon_b - \varepsilon_f] + 1/K_b[\varepsilon_b - \varepsilon_f] \quad (1)$$

The absorption coefficients ε_a, ε_f, and ε_b correspond to A_{obsd}/[DNA], the extinction coefficient for the free complex and the extinction coefficient for the complex in the fully bound form, respectively. The slope and the intercept of the linear fit of the plot of [DNA]/[$\varepsilon_a - \varepsilon_f$] versus [DNA] give 1/[$\varepsilon_a - \varepsilon_f$] and 1/$K_b$[$\varepsilon_b - \varepsilon_f$], respectively. The intrinsic binding constant K_b can beobtained from the ratio of the slope to the intercept (Table. 4) [31]. Emission measurements were carried out by using a JASCO FP-6600 spectrofluorometer. Tris–buffer was used as a blank to make preliminary adjustments. The excitation wavelength was fixed and the emission range was adjusted before measurements. All measurements were made at 20 °C. For emission spectral titrations, complex concentration was maintained constant as 1 μM and the concentration of HS-DNA was varied from 0.05 to 0.5 μM. The emission

enhancement factors were measured by comparing the intensities at the emission spectral maxima under similar conditions. In order to know the mode of attachment of DNA fluorescence quenching experiments of EB-DNA were carried out by adding 0–40 μM palladium(II) complexes to the samples containing10 μM EB, 10 μM DNA and tris-buffer (pH = 7). Before measurements, the system was shook and incubated at room temperature for ~5 min. The emission was recorded at 530–750 nm.

2.7. Bovine serum albumin binding study

The protein binding study was performed by tryptophan fluorescence quenching experiments using bovine serum albumin (BSA, 1 μM) as the substrate in phosphate buffer (pH 7). Quenching of the emission intensity of tryptophan residues of BSA at 346 nm (excitation wavelength at 280 nm) was monitored using complexes **1** and **2** as quenchers with increasing complex concentration. The possible quenching mechanism has been interpreted using the following Stern Volmer Eq. (3), the ratio of the fluorescence intensity in the absence of (I_0) and in the presence of (I_{corr}–corrected fluorescence intensity) the quencher is related to the concentration of the quencher [Q] by a coefficient K_{sv}.

$$I_0/I_{corr} = 1 + K_{SV}[Q] \quad (2)$$

In order to correct the inner filter effect the following Eq. (3), is used.

$$F_{corr} = F_{obs} * 10^{\frac{A_{exc}+A_{em}}{2}} \quad (3)$$

where F_{corr} is the corrected fluorescence value, F_{obs} the measured fluorescence value, A_{exc} the absorption value at the excitation wavelength, and A_{em} the absorption value at the emission wavelength [33].

The binding constant (K_b) and the number of binding sites (n) can be determined according to the method [34] using the Scatchard Eq. (4):

$$\log[(I_0 - I)/I] = \log K_b + n\log[Q] \quad (4)$$

where, K_b is the binding constant for the complex–protein interaction and n is the number of binding sites per albumin molecule, which can be determined by the slope and the intercept of the double logarithm regression curve of log $[(I_0 - I)/I]$ versus log[Q]. Synchronous fluorescence spectra of BSA with various concentrations of complexes were obtained from 300 to 400 nm when $\Delta\lambda$ = 60 nm and from 290 to 500 nm when $\Delta\lambda$ = 15 nm. The excitation and emission slit widths were 5 and 6 nm, respectively. Fluorescence and synchronous measurements were performed using a1 cm quartz cell on JASCO F 6500 spectrofluorimeter.

2.8. DPPH (1,1-diphenyl-2-picryl-hydrazyl) radical scavenging assay

The potential antioxidant activity of new palladium(II) complexes was evaluated by DPPH radical-scavenging assay according to the procedure described previously with a slight modification [35]. DPPH free radicals are used for rapid analysis of antioxidants. While scavenging the free radicals, the antioxidants donate hydrogen and form a stable DPPH-H molecule. Briefly, the various concentrations of the complexes (10–50 mg ml^{-1}) were added to 5 ml of DPPH (0.1 mM in methanol) and were mixed rapidly. Radical scavenging capacity was measured in 10 min intervals using spectrophotometer by monitoring the decrease in absorbance at 517 nm. The IC_{50} values of DPPH decolonization of the complexes were calculated. Butylated hydroxyanisole (BHA) and butylatedhydroxytoluene (BHT) were used as a positive control.

3. Results and discussion

The reactions of H_2L^1 and H_2L^2 with equimolar amount of $[PdCl_2(AsPh_3)_2]$ were carried out in ethanol/dichloromethane mixture (Scheme 1) which afforded two air and light stable complexes. They dissolve in common organic solvents such as dimethylformamide, dimethylsulfoxide, ethanol, methanol, chloroform and dichloromethane. The analytical data of the new complexes agree well with the proposed molecular formulae. The structures of the complexes (**1** and **2**) along with their starting material were confirmed by X-ray crystallographic study.

3.1. IR Spectra

The IR spectra of free Schiff base ligands showed a strong absorption at 1620 and 1640 cm^{-1} corresponding to $\nu_{C=N}$ azomethine group respectively for $[H_2L^1]$ and $[H_2L^2]$. This band has been lowered by 37 and 24 cm^{-1} respectively in the complexes indicating the coordination of azomethine nitrogen atom [16,23]. The medium intensity band appeared at 815–795 cm^{-1} due to $\nu_{C=S}$ of the thiosemicarbazones which has been shifted to 743 cm^{-1} in complex **1** and 738 cm^{-1} in complex **2** indicating the coordination of thiolate sulfur atom after enolisation followed by deprotonation [18]. A broad band corresponding to ν_{OH} appeared at 3419–3423 cm^{-1} in the ligands completely disappeared in the spectra of the new complexes **1** and **2** confirming the coordination of

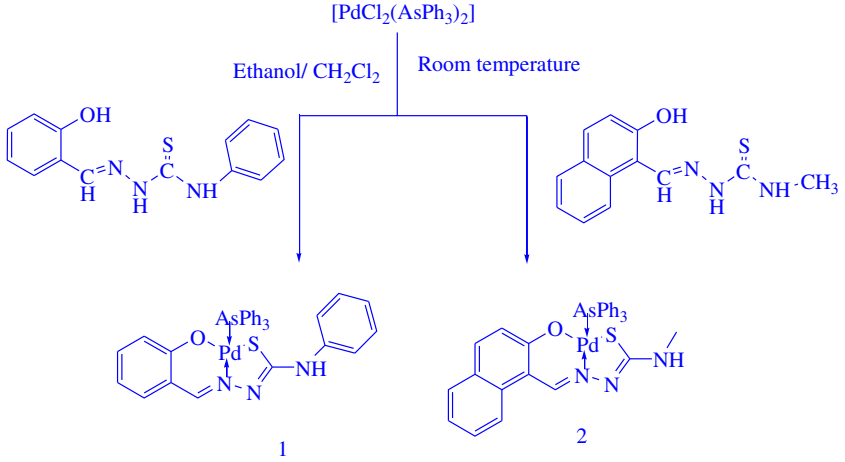

Scheme 1. Preparation of new palladium(II) complexes.

phenolic oxygen after deprotonation. This was further supported by the increase in the value of phenolic C–O stretching frequency from 1270–1250 cm^{-1} to 1342–1259 cm^{-1} [18,22]. In both the complexes the characteristic absorption bands for triphenylarsine were also present in the expectedregion [23].

3.2. Electronic spectra

The electronic spectra of the complexes **1** and **2** have been recorded in dichloromethane and they displayed five to six bands in the region around 240–440 nm. The bands appeared at the region 240-320 nm have been assigned to intra ligand transition and the bands around 340–380 nm have been assigned to ligand to metal charge transfer transition [36,37] . The bands around 440 nm have been assigned to metal to ligand charge transfer transition [38].

3.3. ^1H NMR spectra

The ^{1}H-NMR spectra of H_2L^{1-2} and the corresponding complexes recorded in DMSO showed all the expected signals. In the spectra of H_2L^{1-2}, a singlet appeared in the range 9.11–9.86 ppm has been assigned to N(2)HCS group [20,21]. But in the spectra of the new complexes **1** and **2**, there was no resonance attributable to N(2)H, indicating the coordination of ligands in the anionic form after deprotonation at N(2). A sharp singlet corresponding to the phenolic –OH group has appeared at 11.20–11.41 ppm in the free ligands. But the same singlet has completely disappeared in complexes **1** and **2** confirming the involvement of phenolic oxygen in coordination[17]. In the spectra of H_2L^{1-2} and complexes **1** and **2**, a complex multiplet appeared at 6.60–7.99 ppm due to aromatic protons of ligands and triphenylarsine [18]. Two singlets observed at 8.02–8.35 ppm and 8.40–9.59 ppm has been assigned to azomethine and terminal –NH protons for H_2L^1 and H_2L^2 respectively. Complex **1** showed two singlets at δ 8.6 and 9.6 ppm corresponding to azomethine and terminal –NH protons and complex **2** showed two doublets around δ 8.3 and 9.5 ppm corresponding to azomethine and terminal –NH protons due to the couplingwith a arsine atom of the triphenylarsine and the restricted rotation on the C=N bond of the ligand respectively [20]. In addition, multiplet appeared at δ 2.4 ppm in complex **2** corresponding to methyl group of protons [18]. In the ^{13}C{1H} NMR spectra of the ligands, the thione (C=S) carbon resonates at 186.4 and 181.4 ppm were completely disappeared in the complexes and new resonances at 166.4 and 163.4 ppm indicate the thione to thiol tautomerisation and subsequent thiol coordination. The azomethine carbon resonance is observed at 162.28 and 157.24 ppm in the ligands appeared at 164.0 and 163.48 ppm in the complexes. In both ligands, aromatic carbon atoms of the phenoxy group observed around 152.1–118.19 ppm are almost comparable with the complexes and the literature values [15]. A signal at 28.6 ppm in the ligand H_2L^2 and 27.88 ppm in the complex confirm the presence of methyl group in the system. In both complexes three signals corresponding to the presence of triphenylarsine observed at 153.6, 152.1, and 132.08 ppm (complex 1) and 155.6, 151.4, and 130.12 ppm (complex 2) are in the range of the reported values [15].

3.4. X-ray crystallography

The crystallographic data, selected bond distances and bond angles are listed in Tables 1 and 2. The ORTEP diagrams with numbering scheme of the Palladium precursor and complexes **1** and **2** are in Figs. 1–5. In order to confirm the *trans* configuration of $[PdCl_2(AsPh_3)_2]$ single crystal X-ray structure of this starting complex was solved. The single crystals of $[PdCl_2(AsPh_3)_2]$ were obtained in benzene-acetonitrile medium. The starting complexcrystallizes with one unit of benzene molecule in its lattice. The presence of

Table 1
Crystal data and structure refinement of new Pd(II) thiosemicarbazone complexes.

	$[PdCl_2(AsPh_3)_2]$ CCDC 857204	[Pd(Sal-ptsc)($AsPh_3$)] (**1**) CCDC 857201	[Pd(Nap-mtsc)($AsPh_3$)] (**2**) CCDC 856729
Empirical formula	$C_{39}H_{33}As_2Cl_2Pd$	$C_{32}H_{26}$ AsN_3OPdS	$C_{31}H_{26}As$ N_3OPdS
Formula weight	828.79	681.94	669.93
T (K)	173(2)	173(2)	173(2)
Wavelength (Å)	0.71073	0.71073	0.71073
Crystal system	monoclinic	triclinic	monoclinic
Space group	$P2(1)/n$	$P\bar{1}$	$P2(1)/n$
Unit cell dimensions			
a (Å)	11.651(2)	10.1680(12)	14.0981(3)
b (Å)	18.625(4)	10.5535(12)	11.2881(2)
c (Å)	16.552(3)	13.3852(15)	18.2678(3)
α (°)	90	78.9980(10)	90
β (°)	105.04(3)	82.7610(10)	111.00(10)
γ (°)	90	86.2490(10)	90°
V (Å^3)	3468.8(12)	1397.4(3)	2714.02(9)
Z	4	2	4
D_{calc} (Mg m^3)	1.587	1.621	1.640
Absorption coefficient (mm^{-1})	2.609	1.945	1.640
F(000)	1652	684	1344
Theta range for data collection (°)	1.68–28.34	1.56–28.26	1.58–36.41
Index ranges	$-15 \leqslant h \leqslant 14$, $-24 \leqslant k \leqslant 24$, $-22 \leqslant l \leqslant 22$	$-13 \leqslant h \leqslant 13$, $-13 \leqslant k \leqslant 13$, $-17 \leqslant l \leqslant 17$	$-23 \leqslant h \leqslant 23$, $-18 \leqslant k \leqslant 18$, $-30 \leqslant l \leqslant 30$
Reflections collected/unique	11611/5950[R_{int} = 0.0464]	15607/6261[R_{int} = 0.0433]	42193/13167[R_{int} = 0.0572]
Completeness to theta	28.34 97.6%	28.26 90.4%	36.41 99.5%
Refinement method	Full-matrix least-squares on F^2	Full-matrix least-squares on F^2	Full-matrix least-squares on F^2
Data/restraints/parameters	8458/0/409	6261/0/456	13167/0/344
Goodness-of-fit (GOF) on F^2	0.576	1.046	1.038
Final R indices [$I > 2\sigma(I)$]	R_1 = 0.0218, wR_2 = 0.0662	R_1 = 0.0230, wR_2 = 0.0573	R_1 = 0.0433, wR_2 = 0.0938
R indices (all data)	R_1 = 0.0322, wR_2 = 0.0752	R_1 = 0.0281, wR_2 = 0.0593	R_1 = 0.0845, wR_2 = 0.1081
Largest difference peak and hole (e A^{-3})	0.274 and −1.303	0.330 and −0.539	1.234 and −0.727

Table 2
Selected bond lengths (Å) and angles (°) of new Pd(II) thiosemicarbazone complexes.

$[PdCl_2(AsPh_3)_2]$	[Pd(Sal-ptsc)($AsPh_3$)](1)	[Pd(Nap-mtsc)($AsPh_3$)](2)
Bond lengths		
Pd–Cl1 2.2896(6)	Pd–N9 2.0055(15)	Pd–N1 2.006(19)
Pd–Cl2 2.2738(6)	Pd–O1 2.0064(15)	Pd–O1 2.027(17)
Pd–As1 2.4158(5)	Pd–S1 2.2455(6)	Pd–S1 2.2351(6)
Pd–As2 2.4146(5)	Pd–As1 2.3811(3)	Pd–As1 2.379(3)
Bond angles		
Cl2–Pd–Cl1 178.59(2)	N9–Pd–O1 93.25(6)	N1–Pd–O1 92.18(7)
As2–Pd–As1 176.55(8)	N9–Pd–S1 84.37(5)	N1–Pd–S1 85.08(6)
Cl1–Pd–As1 93.24(14)	O1–Pd–S1 175.70(4)	O1–Pd–S1 177.24(5)
As1–Pd–Cl2 86.36(14)	N9–Pd–As1 176.55(4)	N1–Pd–As1 176.51(5)
Cl2–Pd–As2 91.59(14)	O1–Pd–As1 88.92(4)	O1–Pd–As1 90.91(5)
As2–Pd–Cl1 88.74(14)	S1–Pd–As1 93.63(14)	S1–Pd–As1 91.840(18)

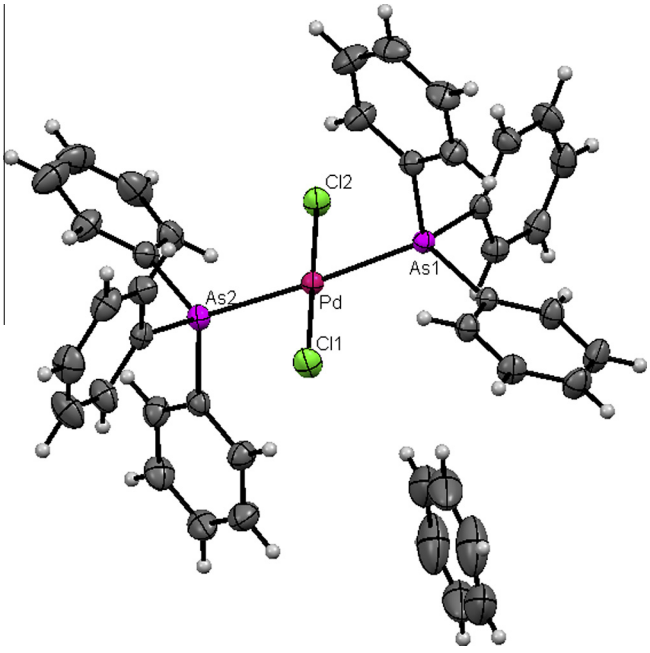

Fig. 1. ORTEP diagram of $[PdCl_2(AsPh_3)_2]\cdot C_6H_6$.

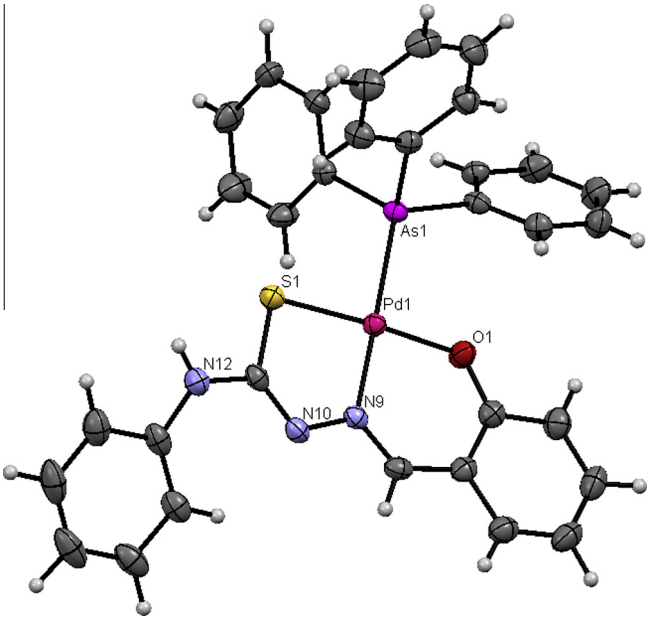

Fig. 2. ORTEP diagram of [Pd(Sal-ptsc)$AsPh_3$] (**1**).

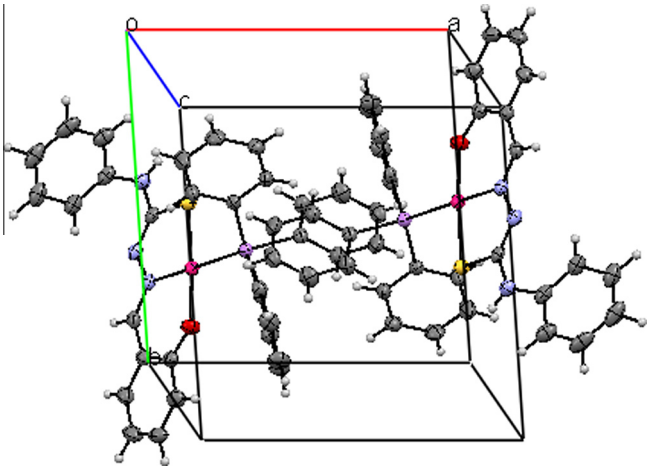

Fig. 3. Molecular Packing diagram of complex **1** along *a* axis.

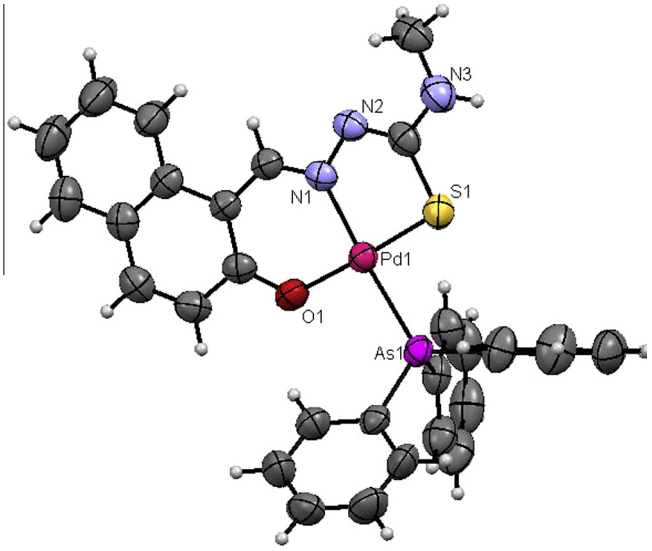

Fig. 4. ORTEP diagram of [Pd(Nap-mtsc)$AsPh_3$] (**2**).

mutually *trans*-triphenylarsine ligands confirm the *trans* configuration of $[PdCl_2(AsPh_3)_2]$. The bond angles for As(1)–Pd–As(2) 176.00(14) and Cl(1)–Pd–Cl(2) 178.59(2) indicates deviation of the geometry from its original square plane. Complex **1** crystallizes in triclinic space group $P\bar{1}$ having two molecules in the unit cell. The molecular packing diagram is given in Fig. 3. In this complex, the ligand is coordinated to palladium as ONS donor by forming one stable five and another six member ring. The remaining coordination site is occupied by triphenylarsine satisfying the fourth coordination site. In this complex, the Pd–O, Pd–As and Pd–S bond lengths of 2.0064(5), 2.3811(3) and 2.2455(6) Å respectively are close to the reported value for palladium(II) complexes [18,20–22]. The Pd–N bond length of 2.0055(15) is almost consistent with the value found for dichlorobis(triphenylarsine)palladium(II) [22]. The triphenylarsine and N(9) nitrogen are mutually *trans* to each other. The basal plane constituted with AsSNO core and the ligand-coordinated to palladium with the bite angle of 84.37° causing considerable deviation from the square planar geometry. The suitable crystals of complex **2** were obtained from dimethylformamide. The complex **2** crystallizes in the monoclinic space group $P2(1)/n$ having four molecules in the unit cell. The packing diagram is given in Fig. 5. In this complex, the ligand coordinated to metal by losing

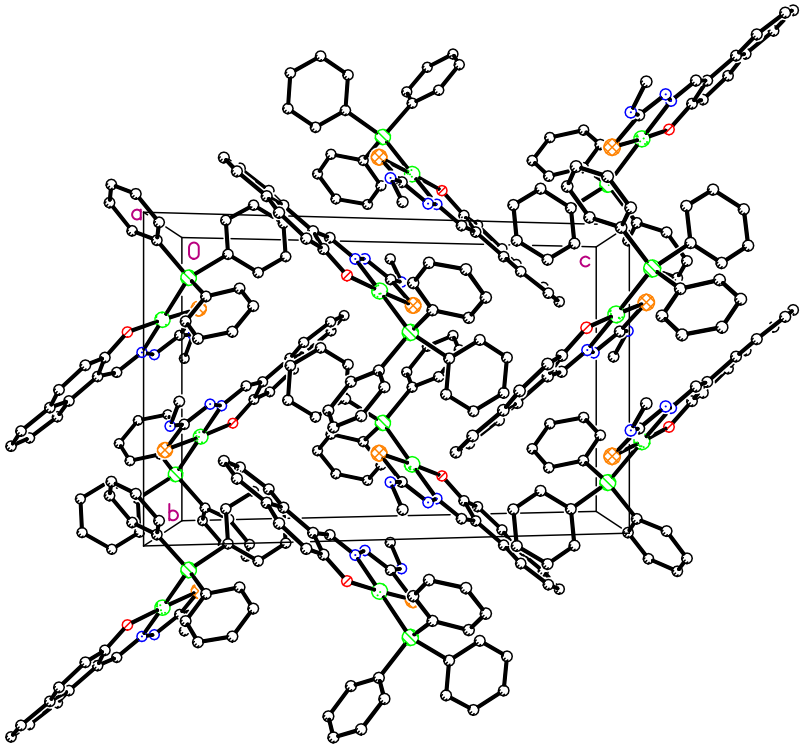

Fig. 5. Molecular packing diagram of complex **2** along the *a*-axis.

Table 3
Electrochemical data of the new palladium(II) complexes.

Complex	Oxidation Pd(II)–Pd(III)				Reduction Pd(II)–Pd(I)				Ligand oxidation				Ligand reduction			
	Epa (V)	Epc (V)	$E_{½}$ (V)	ΔEp (mV)	Epa (V)	Epc (V)	$E_{½}$ (V)	ΔEp (mV)	Epa (V)	Epc (V)	$E_{½}$ (V)	ΔEp (mV)	Epa (V)	Epc (V)	$E_{½}$ (V)	ΔEp (mV)
[Pd(Sal-ptsc)($AsPh_3$)] (**1**)	0.430	0.380	0.455	50	−0.390	−0.320	−0.355	70	1.15	1.25	1.2	100	−1.480	−0.95	−1.23	530
[Pd(Nap-mtsc)($AsPh_3$)] (**2**)	0.672	0.972	0.822	300	−0.560	−0.480	−0.520	80	–	–	–	–	–	–	–	–

two protons from its tautomeric thiol form and phenolic –OH. They act as binegative tridentate ligands via the mercapto sulphur, phenolic oxygen and β-nitrogen atoms by forming one six and another five member ring with bite angle of 84.37(5)° [N(9)–Pd(1)–S(1)]. The Pd–N 2.0062(19) Å, Pd–S 2.2351(6) Å, Pd–O 2.0270(17) Å and Pd–As 2.3790(3) Å bond lengths are in the expected region and agreevery well with the already reported values [18,20–22]. The complex has the bite angle of 85.06(6) in the PdNSOAs square planar core. The two *trans* angles O(1)–Pd–S(1) 177.24(5) and N(1)–Pd(1)–As(1) 176.51(5) deviate considerably from the ideal angle causing significant distortion in the square plane of the complex **2**.

3.5. Electrochemistry

Electrochemical studies of the new palladium(II) complexes have been done in dichloromethane medium by using platinum wire working electrode and platinum disc counter electrode. All the potentials were referenced to Ag/AgCl electrode. Ferrocene was used as an external standard. Voltammetric data are presented in Table 3. Complex **1** exhibited one electron reversible oxidation and reduction corresponding to Pd(II)–Pd(III) and Pd(II)–Pd(I) at $E_{1/2}$ of 0.455 V with the peak to peak separation of 50 and −0.355 V with the peak to peak separation of 70 mV respectively.

Table 4
Binding constant for interaction of complexes (**1** and **2**) with HS-DNA.

System	K_b ($\times 10^4$ M^{-1})
HS-DNA + **1**	1.68 ± 0.15
HS-DNA + **2**	1.92 ± 0.57

In addition, it exhibited a reversible ligand oxidation and quasi-reversible ligand reduction at $E_{1/2}$ of 1.20 and −1.23 Vwith the peak to peak separation of 100 and 530 mV respectively. The complex **2** showed a one electron quasi-reversible oxidation corresponding to Pd(II)–Pd(III) and one electron reversible reduction corresponding to Pd(II)–Pd(I) with a peak to peak separation of 300 and 80 mV respectively with the potentials of 0.822 and −0.520 V. The adsorption of the complex on to the electrode surface or slow electron transfer may be the reason for quasi- reversible electron transfer process [39].

3.6. DNA binding studies

3.6.1. Electronic absorption titration

The application of electronic absorption spectroscopy is one of the most useful techniques for DNA-binding properties. The

absorption spectra of two new palladium (II) complexes (1 μM) in the absence and presence of Herring Sperm HS-DNA (0.05–0.50 μM) are recorded, and the absorption spectra of the three complexes are given in Fig. 6. The absorption spectra of complex **1** consists of three resolved bands [Intra ligand (IL) and Metal to ligand (MLCT) transitions] centered at 250 nm (IL), 389 and 406 nm (MLCT). As the DNA concentration is increased, the hyperchromism (A = 0.2825–2.800) with a red shift of 12 nm (up to 262 nm) was observed in the IL band. The MLCT bands at 389 and 406 nm showed modest hypochromism (A = 0.0937–0.0927 and A = 0.0978–0.0949 respectively) with negligible shifts in the wavelength. The binding behavior of complex **2** is quite different. It exhibited hyperchromism at 268 nm (A = 0.0368–1.770) with 5 nm blue shift. In addition, three resolved charge transfer transitions (CT) centered at 342, 421 and 475 nm showed modest hypochromism with negligible shifts in the wavelength. The observed hyperchromic effect with red/blue shift suggested that the new complexes bind to CT-DNA by external contact, possibly due to

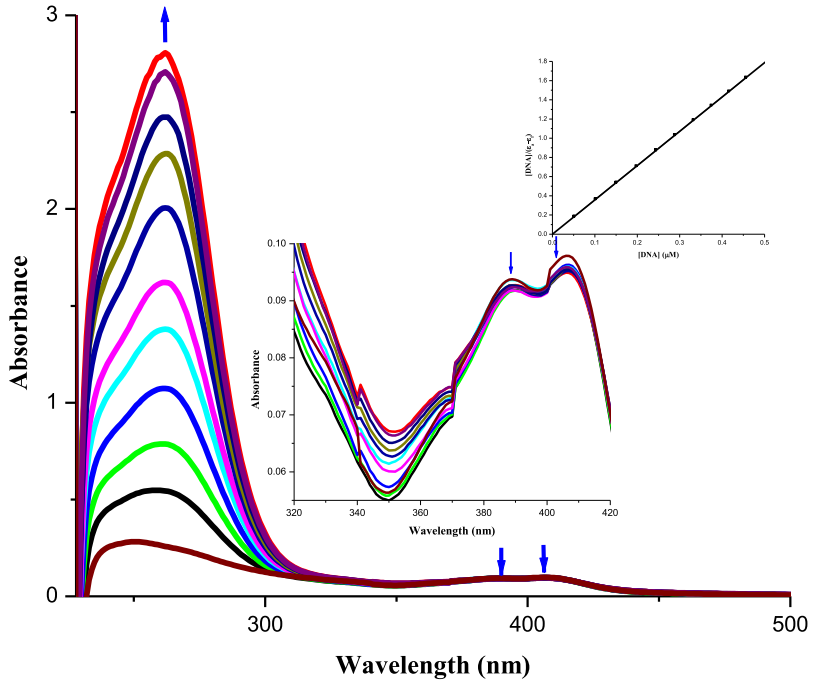

(1)

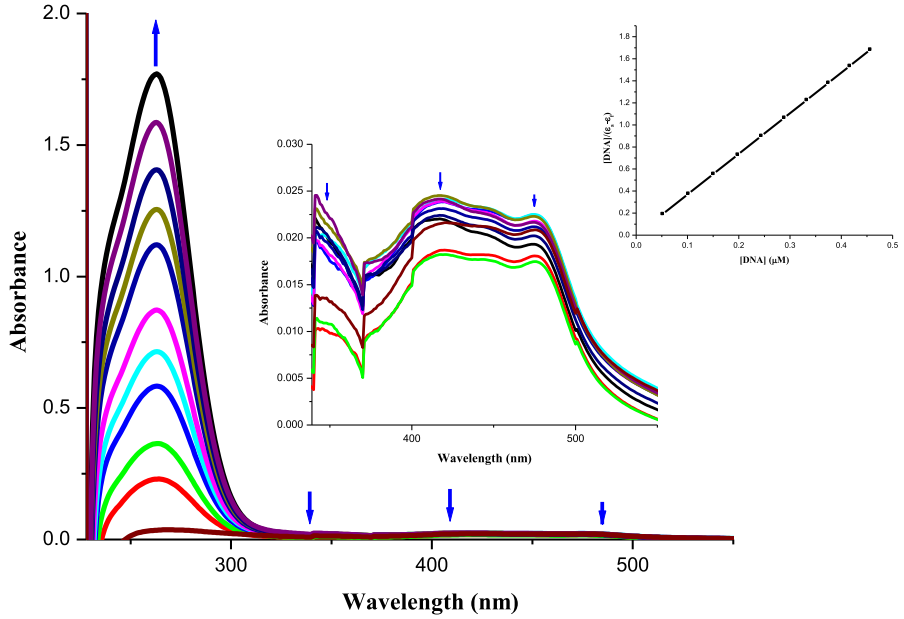

(2)

Fig. 6. Absorption titration spectra of **1** and **2** with increasing concentrations (0.05–0.5 μM) of HS-DNA (tris HCl buffer, pH 7); the inset shows binding isotherms with HS-DNA.

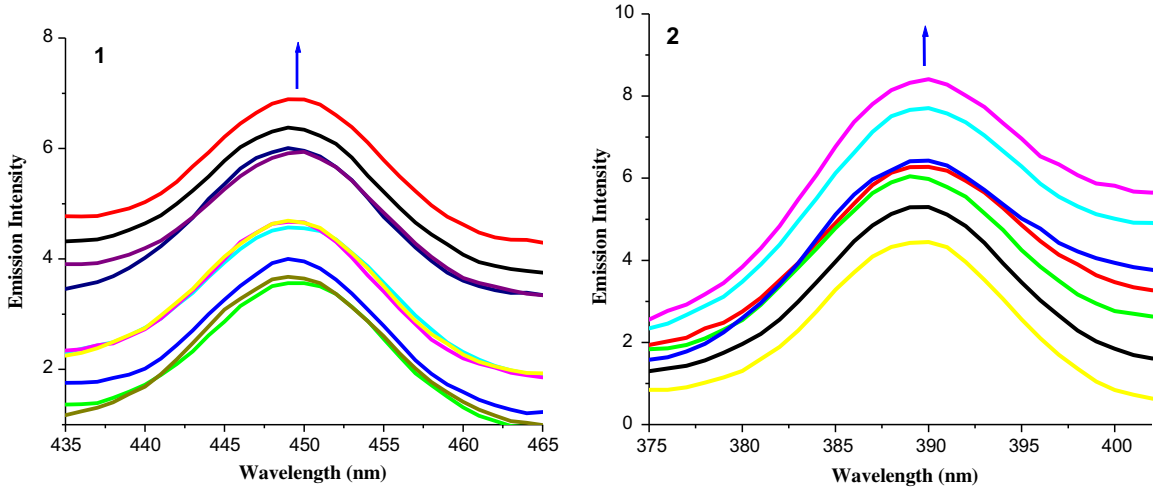

Fig. 7. Changes in the emission spectra of **1** and **2**, with increasing concentrations (0.05–0.5 μM) of HS-DNA (tris HCl buffer, pH 7);

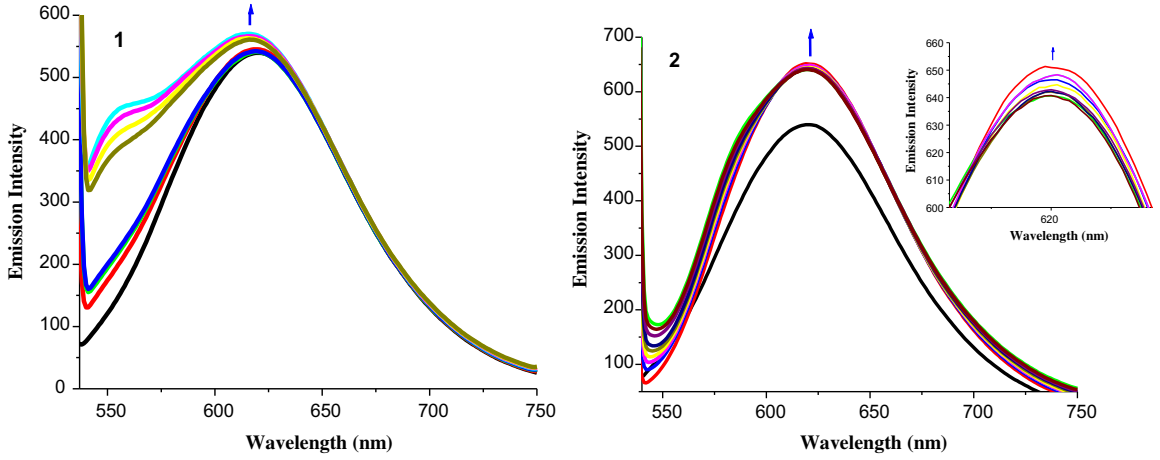

Fig. 8. The emission spectra of the DNA–EB system (λ_{exc} = 515 nm, λ_{em} = 530–750 nm), in the presence of complexes **1** and **2**. [DNA] = 10 μM, [Complex] = 0–40 μM, [EB] = 10 μM. The arrow shows the emission intensity changes upon increasing complex concentration.

electrostatic binding [40]. The intrinsic binding constant K_b can be determined by monitoring the changes in the absorbance in the IL band at the corresponding λ_{max} with increasing concentration of DNA and is given by the ratio of slope to the Y intercept in plots of [DNA]/($\varepsilon_a - \varepsilon_f$) versus [DNA] (Insets in Fig. 6, Table 4). From the binding constant values, it is inferred that the complex **2** exhibited better binding than **1**.

In the emission spectra, Complexes **1** and **2** had fluorescence at 450 and 390 nm respectively. If HS-DNA solution was added to this complex solution, fluorescence intensity was increased without any shift in wavelengths (Fig. 7). The enhanced fluorescence intensity observed for the complexes represents electrostatic binding mode of HS-DNA.

3.6.2. Competitive studies with ethidium bromide

The competitive EB binding studies may be carried out in order to examine the binding of complexes with HS-DNA. Emission spectra of EB bound to HS-DNA in the absence and presence of complexes **1** and **2** have been recorded. The fluorescence emission intensities of EB bound to HS-DNA at 620 nm showed increasing trend with increasing concentration of the complexes showed in Fig. 8, indicating that they cannot displace EB from the DNA-EB complex. This observation is often considered that they can bind weakly to the DNA probably by electrostatic interaction.

3.7. Quenching mechanism of BSA by complexes

3.7.1. UV absorption spectra of BSA in the presence of complexes (*1* and *2*)

UV absorption spectrum is a very simple and applicable method to explore the structural change, to know the complex formation in solution and is useful to distinguish the type of quenching exist i.e., static or dynamic quenching [41]. The UV absorption spectra of BSA in the presence of different concentrations of two complexes (Fig. 9) showed that the absorption intensity of BSA was enhanced with the addition of these complexes. There was a little blue shift of complex–BSA spectrum (from 280 to 277 nm). This phenomenon indicates the interaction of BSA with the compounds [42]. It is well known that dynamic quenching only affects the excited state of fluorophore and does not change the absorption spectrum. However, the formation of non-fluorescence ground-state complex induced the change in absorption spectrum of fluorophore. Thus, possible quenching mechanism of BSA by **1** and **2** was a static quenching process [43] .

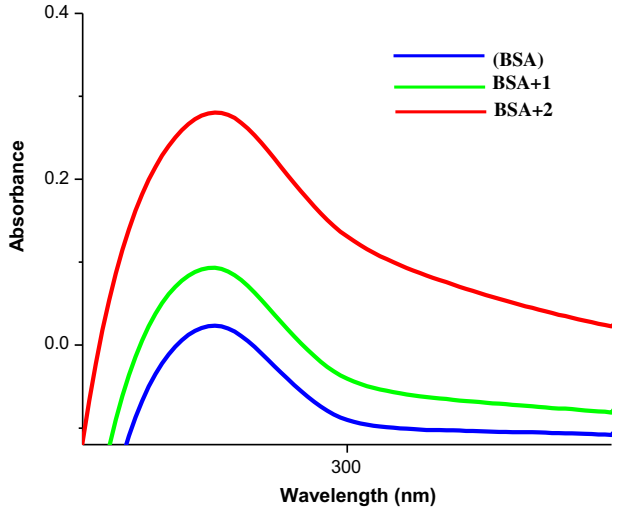

Fig. 9. Absorption spectra of absence and presence of complexes with BSA (1×10^{-5} M).

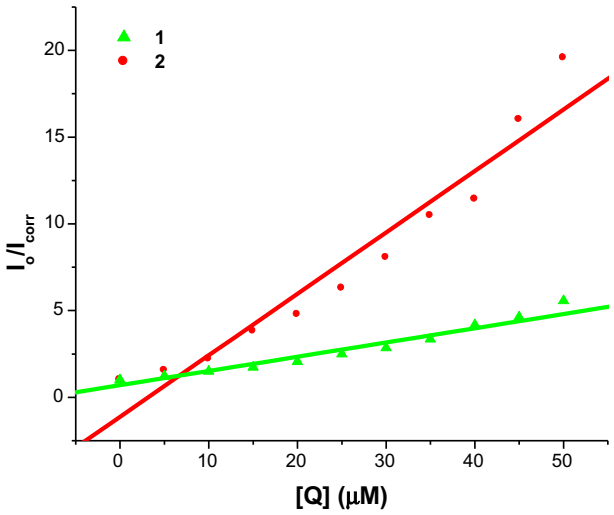

Fig. 11. Plot of I_0/I vs. [Q].

3.7.2. Fluorescence quenching studies of BSA

Serum albumin (SA) is the most abundant protein in plasma and is involved in the transport of drugs, metal ions, and compounds through the bloodstream. Bovine serum albumin (BSA) is the most extensively studied serum albumin, due to its structural homology with human serum albumin (HSA). Binding to these proteins may lead to loss or enhancement of the biological properties of the original drug, or provide paths for drug transportation. Since serum albumins are well known to bind small aromatics, the possible binding interactions of the palladium(II) salicylaldehyde and 2-hydroxy 1-naphthaldehyde thiosemicarbazone complexes with BSA have been investigated by emission-titration experiments at room temperature. A solution of BSA (1 μM) was titrated with various concentrations of the complexes (0–50 μM). Fluorescence spectra were recorded in the range of 290–450 nm upon excitation at 280 nm. Thechanges observed on the fluorescence emission spectra of a solution of BSA on the addition of increasing amounts of the complexes are shown in Fig. 10. Upon the addition of complexes **1** and **2** to BSA, a significant decrease of the fluorescence intensity of BSA at 346 nm from the initial fluorescence intensity was observed accompanied by a red shift of 2 and 10 nm, respectively. The observed quenching may be attributed to possible changes in protein secondary structure leading to changes in the tryptophan environment of BSA, thus indicating binding of each

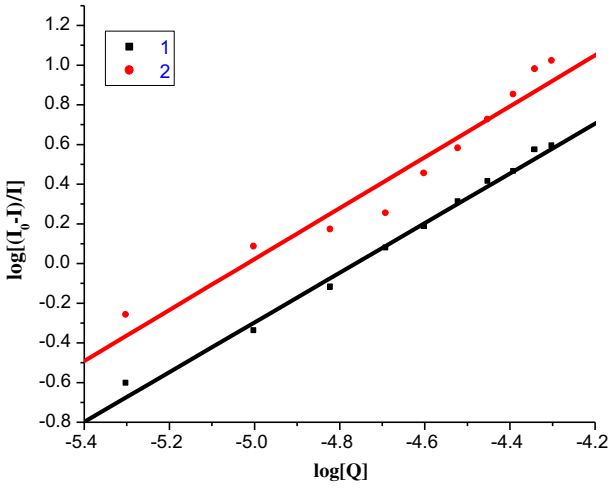

Fig. 12. Plot of $\log[(F_0 - F)/F]$ vs. $\log[Q]$.

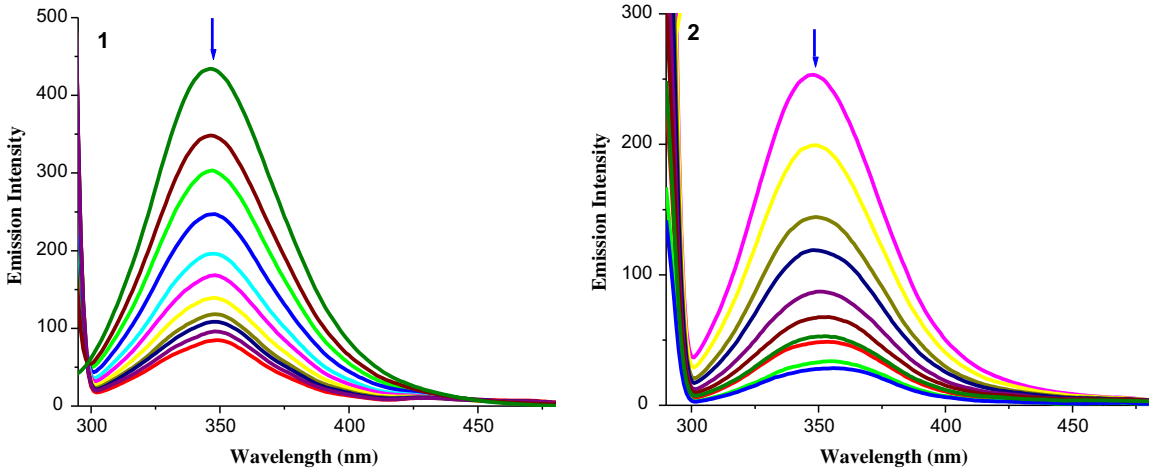

Fig. 10. The emission spectra of BSA (1 μM; λ_{exc} = 280 nm; λ_{emi} = 346 nm) in the presence of increasing amounts of complexes **1** and **2** (0–50 μM). The arrow shows the emission intensity changes upon increasing complex concentration.

Table 5
Quenching constant (K_q), binding constant (K_{bin}) and number of binding sites (n) for the interactions of complexes **1** and **2** with BSA.

Complex	K_q/M^{-1}	K_{bin}/M^{-1}	n
1	$8.2 \pm 0.24 \times 10^4$	$9.2 \pm 0.43 \times 10^5$	1.25
2	$3.5 \pm 0.35 \times 10^5$	$2.7 \pm 0.19 \times 10^6$	1.28

complex to BSA [44]. The K_q value obtained from the plot of I_0/I_{corr} versus [Q] (2)was found to be 8.2×10^4 and 3.5×10^5 M^{-1} corresponding to complexes **1** and **2** respectively. The observed linearity in the plots (Fig. 11) indicated the ability of the complexes to quench the emission intensity of BSA. The strong protein-binding ability of **2** with enhanced hydrophobicity is consistent with its strong DNA binding affinity.

3.7.3. Binding constants and the number of binding sites

For the static quenching interaction, if it is assumed that there are similar and independent binding sites in the biomolecule, the binding constant K_b and the number of binding sites per albumin molecule n were determined by the slope and the intercept of the double logarithm regression curve of log $[(I_0 - I)/I]$ versus log[Q] Eq. (4) (Fig. 12; Tables 5). The values of n at room temperature are approximately equal to **1**, which indicates that there is just one single binding site in BSA for the complexes **1** and **2**.

3.7.4. Synchronous fluorescence spectroscopic studies of BSA

Synchronous fluorescence spectral study was used to obtain information about the molecular environment in the vicinity of the fluorophore moieties of BSA [45]. When the difference ($\Delta\lambda$) between the excitation and emission wavelengths is fixed at 15 and 60 nm, and the amount of complexes added to BSA (1 μM) is increased, a large decrease in fluorescence intensity with a red-shift in the tryptophan emission maximum is observed (Fig. 13). In contrast, the emission intensity of tyrosine residue increases with red shift in the emission maximum (Fig. 14). The observation indicated that complexes mainly bind to tryptophan residues of BSA. It indicates that the hydrophobicity of microenvironment around tryptophan residues decreases in the presence of the complexes [46].

3.8. DPPH radical-scavenging assay

The free radical scavenging activity of new Pd(II) complexes was tested by its ability to bleach the stable radical DPPH. This

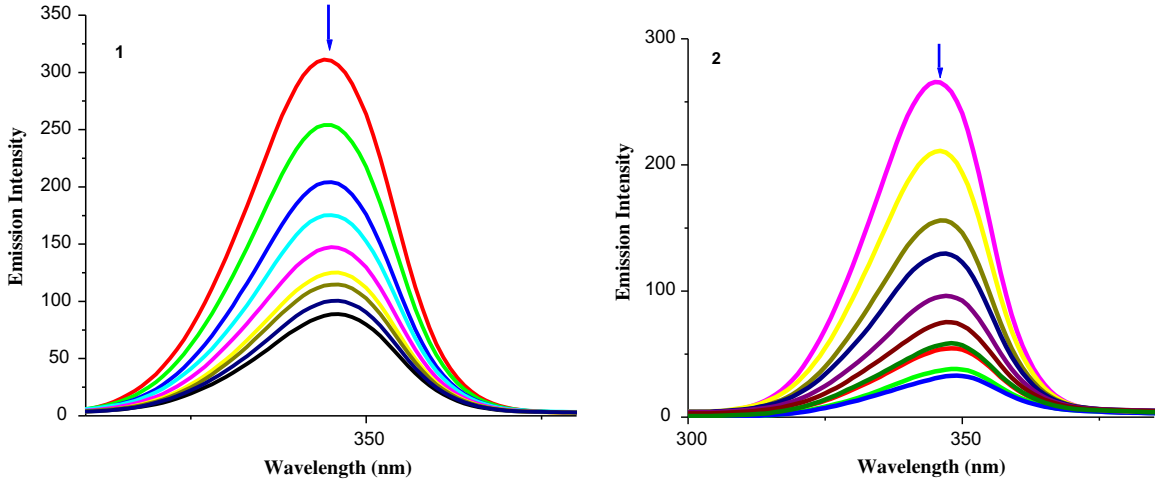

Fig. 13. Synchronous spectra of BSA (1 μM) in the presence of increasing amounts of complexes **1** and **2** (0–50 μM) for a wavelength difference of $\Delta\lambda$ = 60 nm. The arrow shows the emission intensity changes upon increasing concentration of complex.

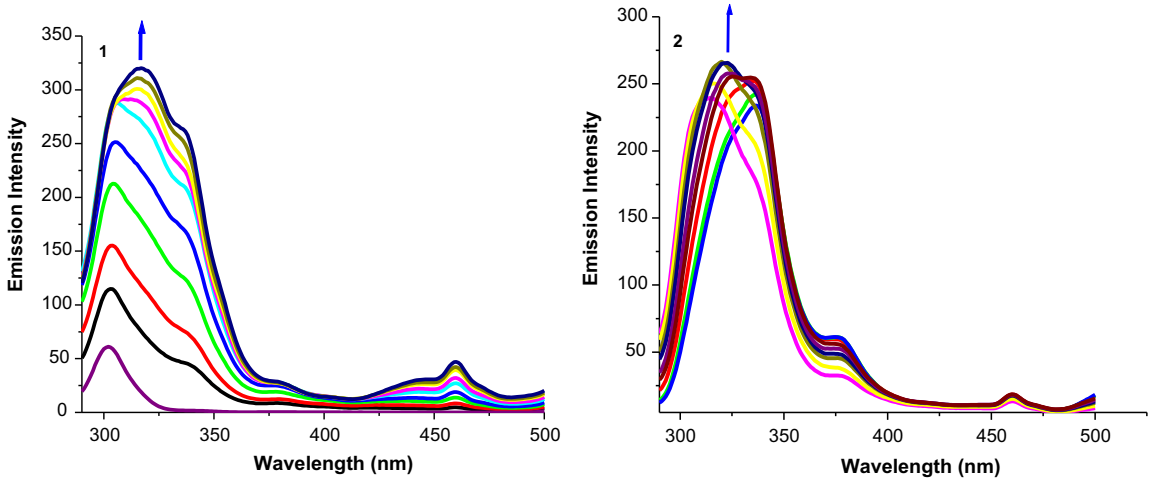

Fig. 14. Synchronous spectra of BSA (1 μM) in the presence of increasing amounts of complexes **1** and **2** (0–50 μM) for a wavelength difference of $\Delta\lambda$ = 15 nm. The arrow shows the emission intensity changes upon increasing concentration of complex.

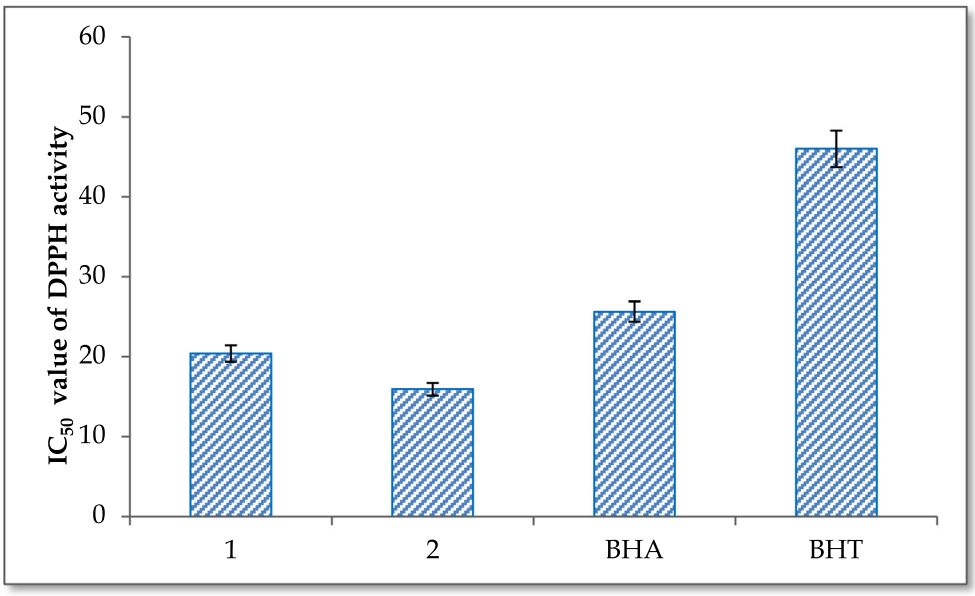

Fig. 15. DPPH inhibition activity of complexes **1** and **2**.

Table 6
IC_{50} values (μM) calculated from DPPH assay of Pd(II) complexes **1**, **2** and standards (BHA and BHT).

Complex	DPPH (IC_{50} in μM)
1	20.40 ± 0.24
2	15.91 ± 0.21
BHA	25.60 ± 0.12
BHT	45.97 ± 0.26

assay provided information on the reactivity of the compound with a stable free radical. Because of the odd electron, DPPH shows a strong absorption band at 517 nm in the visible spectrum [35]. As this electron becomes paired off in the presence of a free radical scavenger, the absorption vanishes, and the resulting decolonization is stoichiometric with respect to the number of electrons taken up. The new palladium(II) complexes exhibited good DPPH radical-scavenging effect higher than that of butylated hydroxyanisole (BHA) and butylated hydroxytoluene (BHT). The free radical scavenging activity of the complexes increased with an increase in the concentration of the complex and it is measured interms of IC_{50} values (Fig. 15; Table 6) which is an encouraging sign for this complex to be a good anti-cancer drug. The observed antioxidant activity of the palladium complexes may be due to the neutralization of the free radical character of DPPH either by transfer of an electron or a hydrogen atom [47].

4. Conclusion

New palladium(II) complexes containing salicylaldehyde-4(N)-phenylthiosemicarbazone and 2-hydroxy-1-naphthaldehyde-4(N)-methylthiosemicarbazone have been synthesized and characterized by various spectro analytical techniques. The structures were confirmed by X-ray diffraction studies. In addition, the structure of the palladium precursor $[PdCl_2(AsPh_3)_2]$ has also been solved. The new complexes were introduced to study their interaction with DNA and protein by taking Herring Sperm (HS-DNA) and protein BSA as models and found significant activities on them. The complexes exhibited better DPPH radical scavenging activity than the conventional standards BHA and BHT. In general, by comparing the activities of complex **1** and **2**, the latter exhibited better activity than former and this may be due to the presence of stronger electron withdrawing naphthoxy group in **2**,favors more electron deficiency on palladium(II) metal centre which increases the efficacy of free radical scavenging than that of the phenoxy complex **1**.

Acknowledgment

The authors gratefully acknowledge **Department of Science and Technology, India** and **Council of Scientific and Industrial Research, India** for their financial assistance.

Appendix A. Supplementary material

Supplementary data associated with this article can be found, in the online version, at http://dx.doi.org/10.1016/j.ica.2013.06.038.

References

[1] (a) D.X. West, S.B. Padhye, P.B. Sonaware, Struct. Bonding (Berlin) 76 (1991) 4;
(b) S.B. Padhye, G. Kauffman, Coord. Chem. Rev. 63 (1985) 127;
(c) D.X. West, A.E. Liberta, S.B. Padhye, R.C. Chikate, P.B. Sonawane, A.S. Kumbhar, R.G. Yerande, Coord. Chem. Rev. 123 (1993) 49;
(d) J.S. Casas, M.S. Garcia-Tasende, J. Sordo, Coord. Chem. Rev. 209 (2000) 197;
(e) M.J.M. Campbell, Coord. Chem. Rev. 15 (1975) 279;
(f) D.S. Kalinowski, D.R. Richardson, Pharmacol. Rev. 57 (2005) 547;
(g) H. Beraldo, D. Gambino, Mini-Rev. Med. Chem. 4 (2004) 31;
(h) M.J. Clarke, F. Zhu, D.R. Frasca, Chem. Rev. 99 (1999) 2511;
(i) A.G. Quiroga, C. Navarro-Ranninger, Coord. Chem. Rev. 248 (2004) 119;
(j) I. Bettina, H.B. Gray, S.J. Lippard, J.S. Valentine, Bioinorganic Chemistry, University Science Books, MillValley, CA, 1994;
(k) W. Kaim, B. Schewederski, Bioinorganic Chemistry: Inorganic Elements in the Chemistry of Life, Wiley, New York, 1994.
[2] D.K. Demertzi, A. Domopoulou, M.A. Demertzis, G. Valle, A. Papageorgiou, J. Inorg. Biochem. 68 (1997) 147.
[3] D.K. Demertzi, M.A. Demertzis, V. Voragi, Chemotherapy 44 (1998) 421.
[4] D.X. West, J.K. Swearingen, A.K. El-Sawaf, Transition Met. Chem. 25 (2000) 87.
[5] A. Castineiras, I. Garcia, E. Bermejo, D.X. West, Z. Naturforsch. 55b (2000) 511.
[6] A. Castineiras, I. Garcia, E. Bermejo, D.X. West, Polyhedron 19 (2000) 1873.
[7] (a) B.M. Zeglis, V.C. Pierre, J.K. Barton, Chem. Commun. (2007) 4565;
(b) D.S. Sigman, A. Mazumder, D.M. Perrin, Chem. Rev. 93 (1993) 2295.
[8] (a) J.G. Vos, J.M. Kelly, Dalton Trans. (2006) 4869;
(b) K.E. Erkkila, D.T. Odom, J.K. Barton, Chem. Rev. 99 (1999) 2777;
(c) C. Moucheron, A. Kirsch-De Mesmaeker, J.M. Kelly, J. Photochem. Photobiol., B 40 (1997) 91;

(d) M.J. Hannon, Chem. Soc. Rev. 36 (2007) 280;
(e) C. Metcalfe, J.A. Thomas, Chem. Soc. Rev. 32 (2003) 215.
[9] R.A. Finch, M.C. Liu, S.P. Grill, W.C. Rose, R. Loomisa, K.M. Vasquez, Y.C. Cheng, A.C. Sarforelli, Biochem. Pharmacol. 59 (2000) 983.
[10] A.I. Matesanz, J.M. Perez, P. Navarro, J.M. Moreno, E. Colacio, P. Souza, J. Inorg. Biochem. 76 (1999) 29.
[11] D. Kovala-Demertzi, M.A. Demertzis, J.R. Miller, C. Papadopoulou, C. Dodorou, G. Filousis, J. Inorg. Biochem. 86 (2001) 555.
[12] A.R. Jalilian, M. Sadeghi, Y.Y. Kamrani, Radiochim. Acta 94 (2006) 865.
[13] S. Padhye, Z. Afrasiabi, E. Sinn, J. Fok, K. Mehta, N. Rath, Inorg. Chem. 44 (2005) 1154.
[14] N. Bharti, F. Athar, M.R. Maurya, A. Azam, Bioorg. Med. Chem. 12 (2004) 4679.
[15] P. Kalaivani, R. Prabhakaran, P. Poornima, F. Dallemer, K. Vijayalakshmi, V. Vijaya Padma, K. Natarajan, Organometallics 31 (2012) 8323. and reference cited there in.
[16] R. Prabhakaran, R. Karvembu, T. Hashimoto, K. Shimizu, K. Natarajan, Inorg. Chim. Acta 358 (2005) 2093.
[17] R. Prabhakaran, P. Kalaivani, R. Jayakumar, M. Zeller, A.D. Hunter, S.V. Renukadevi, E. Ramachandran, K. Natarajan, Metallomics 3 (2011) 42.
[18] R. Prabhakaran, S.V. Renukadevi, R. Karvembu, R. Huang, J. Mautz, G. Huttner, R. Subhaskumar, K. Natarajan, Eur. J. Med. Chem. 43 (2008) 268.
[19] R. Prabhakaran, S.V. Renukadevi, R. Karvembu, R. Huang, M. Zeller, K. Natarajan, Inorg. Chim. Acta 361 (2008) 2547.
[20] P. Kalaivani, R. Prabhakaran, F. Dallemer, P. Poornima, E. Vaishnavi, E. Ramachandran, V. Vijaya Padma, R. Renganathan, K. Natarajan, Metallomics 4 (2012) 101.
[21] P. Kalaivani, R. Prabhakaran, E. Ramachandran, F. Dallemer, G. Paramaguru, R. Renganathan, P. Poornima, V. Vijaya Padma, K. Natarajan, Dalton Trans. 41 (2012) 2486.
[22] R. Prabhakaran, P. Kalaivani, R. Huang, M. Sieger, W. Kaim, P. Viswanathamurthi, F. Dallemer, K. Natarajan, Inorg. Chim. Acta 376 (2011) 317.
[23] R. Prabhakaran, C. Jayabalakrishnan, V. Krishnan, K. Pasumpon, D. Sukanya, Appl. Organomet. Chem. 20 (2006) 203.
[24] R. Prabhakaran, P. Kalaivani, P. Poornima, F. Dallemer, G. Paramaguru, V. Vijaya Padma, R. Renganathan, K. Natarajan, Dalton Trans. 41 (2012) 9323.
[25] R. Prabhakaran, P. Kalaivani, R. Huang, P. Poornima, V. Vijaya Padma, F. Dallemer, J. Biol. Inorg. Chem. 18 (2013) 233.
[26] S. Purohit, A.P. Kolay, L.S. Prasad, P.T. Manoharan, S. Ghosh, Inorg. Chem. 28 (1989) 3735.
[27] J.L. Burmeester, F. Basolo, Inorg. Chem. 3 (1964) 1587.
[28] A.I. Vogel, Text book of Practical organic Chemistry, fifth ed., Longman, London, 1989. 268.
[29] G.M. Sheldrick, SHELXTL Version 5.1, An Integrated System for Solving, Refining and Displaying Crystal Structures from Diffraction Data, Siemens Analytical X-ray Instruments, Madison, WI, 1990.
[30] G.M. Sheldrick, SHELXL-97, A Program for Crystal Structure Refinement Release 97-2, Institut fur Anorganische Chemie der Universitat Gottingen, Tammanstrasse 4, D-3400, Gottingen, Germany, 1998.
[31] A. Wolfe, G.H. Shimer, T. Meehan, Biochemistry 26 (1987) 6392.
[32] G. Cohen, H. Eisenberg, Biopolymers 8 (1969) 45.
[33] M. van de Weert, L. Stella, J. Fluoresc. 20 (2010) 625.
[34] M. Jiang, M.X. Xie, D. Zheng, Y. Liu, X.Y. Li, X. Chen, J. Mol. Struct. 692 (2004) 71.
[35] M.S. Blios, Nature 26 (1958) 1199.
[36] Y.P. Tiam, C.Y. Duan, Z.L. Lu, X.Z. You, Polyhedron 15 (1996) 2263.
[37] S. Dey, V.K. Jain, A. Kwoedler, W. Kaim, Indian J. Chem. 42A (2003) 2339.
[38] D.M. Boghaei, S. Mohebi, J. Chem. Res. (2001) 224.
[39] A.W. Wallace, W.R. Murphy, J.D. Peterson, Inorg. Chim. Acta 166 (1989) 47.
[40] E.C. Long, Biochemistry 22 (1983) 251.
[41] Y.J. Hu, Y. Liu, J.B. Wang, X.H. Xiao, S.S. Qu, J. Pharm. Biomed. Anal. 36 (2004) 915.
[42] Y.Y. Yue, X.G. Chen, J. Qin, X.J. Yao, Dyes Pigm. 79 (2008) 176.
[43] H.Y. Liu, Z.H. Xu, Chem. Pharm. Bull. 57 (2009) 1237.
[44] Y. Wang, H. Zhang, G. Zhang, W. Tao, S. Tang, J. Lumin. 126 (2007) 211.
[45] N. Wang, L. Ye, B.Q. Zhao, J.X. Yu, Braz. J. Med. Biol. Res. 41 (2008) 589.
[46] B. Liu, Y. Guo, J. Wang, R. Xu, X. Wang, D. Wang, L.Q. Zhang, Y.N. Xu, J. Lumin. 130 (2010) 1036.
[47] G.H. Naik, K.I. Priyadarsini, J.G. Satav, M.M. Banavalikar, P.P. Sohoni, M.K. Biyani, Phytochemistry 63 (2003) 97.